AJNR Am J Neuroradiol 22:305–310, February 2001

Identification and Anatomic Description of the Anterior Choroidal Artery by Use of 3D-TOF Source and 3D-CISS MR Imaging

Martin Wiesmann, Indra Yousry, Klaus C. Seelos, and Tarek A. Yousry

BACKGROUND AND PURPOSE: **The importance of the anterior choroidal artery (AChA) is related to its supply of crucial anatomic structures, such as the internal capsule. Angiographically, the AChA can be detected in 71% to 98% of patients, but as yet, its visibility on MR images has not been evaluated. Our goal was to assess the sensitivity of MR imaging in the identification of the AChA and its anatomic characteristics.**

METHODS: **Twenty volunteers underwent MR imaging with a 3D time-of-flight (3D-TOF) sequence, 10 of them additionally with a 3D Fourier transformation constructive interference in steady state (3D-CISS) sequence. The MR angiographic source images and the 3D-CISS images were analyzed independently by two neuroradiologists, who evaluated the ability to identify the different segments of the AChA and the posterior communicating artery (PComA) according to a previously defined scoring system (0 = not identified, 1 = most probably identified, 2 = identified with certainty). Additionally, three patients were examined who had an arteriovenous malformation (AVM) supplied by the AChA.**

RESULTS: **In the volunteers, the PComA was identified with certainty in 87.5% on 3D-TOF sequences and in 95% on 3D-CISS sequences; the AChA was identified with certainty in 92.5% on 3D-TOF sequences and in 90% on 3D-CISS sequences. 3D-CISS images showed additional anatomic information in six of 20 vessels. In the three patients, the enlarged AChA was identified with certainty on both imaging sequences.**

CONCLUSION: **The AChA can be reliably identified using both 3D-CISS sequences and the source images of the 3D-TOF sequence. MR imaging can be used to assess and follow-up AChA-related disorders, especially AVMs.**

The importance of the anterior choroidal artery (AChA) is related to its strategic and extensive area of supply. Although the AChA territory shows large variations, the most consistent area contains the optic tract, the posterior limb of the internal capsule, the cerebral peduncle, and the choroid plexus (1–4). In 1925, Foix et al (5) described the AChA syndrome, which includes, in its complete form, the triad of hemiplegia, hemisensory loss, and hemianopia. However, incomplete forms are more frequent (6).

Additionally, the artery may be involved in cases of intracranial aneurysms, arteriovenous malformations (AVMs), or intracranial tumors. Therefore, diagnostic evaluation of the AChA is required in several neurologic conditions. Because of its noninvasiveness, MR angiography could be the first choice for studying intracranial vessels, although, until recently, this technique has been considered not sensitive enough to study small arteries, such as the AChA. Another MR imaging technique used to visualize fine structures is the 3D Fourier transformation constructive interference in steady state (3D-CISS) sequence. The effect of this sequence may be best described as MR cisternography, and it has been used successfully to identify small nerves and vessels located in the cisterns (7).

The goals of our study were to determine the sensitivity of MR angiography in identifying the AChA by using a time-of-flight (TOF) sequence and a 3D-CISS sequence and to assess the anatomic course of the AChA by using MR imaging.

Methods

Subjects

Twenty healthy subjects (nine men and 11 women, 23–63 years old; mean age, 40 ± 13 years) were included in the

Received March 27, 2000; accepted after revision July 27.

Presented in part at the annual meeting of the American Society of Neuroradiology, San Diego, May 1999.

From the Department of Neuroradiology, Klinikum Grosshadern, Marchioninistr. 15, D-81377 Munich, Germany.

Address reprint requests to Tarek A. Yousry, MD.

FIG 1. *A–C,* Axial MR angiographic source images through the midbrain of a 31-year-old male volunteer obtained using a 3D-TOF sequence (31/7/1) with 0.81 mm between images and displayed from caudal (*A*) to cranial (*C*). The AChA can be seen bilaterally. The left AChA (*long arrow*) is visible from its point of origin from the carotid artery (*A*) throughout its cisternal segment (*A* and *B*) and as it runs along the medial aspect of the uncus and curves laterally along the medial aspect of the temporal lobe (gyrus ambiens) before crossing the cisterna ambiens to enter the choroidal fissure (*C*). The AChA on the right side (*short arrow*) is visible at its origin (*B*) and along its cisternal course (*C*).

FIG 2. *A* and *B,* Axial MR source images through the midbrain of a 27-year-old male volunteer obtained using the 3D-CISS sequence (12.3/5.9/1) with a distance of 1.32 mm between slices and displayed from caudal (*A*) to cranial (*B*). The PComA and AChA can be identified bilaterally. The right AChA (*B, straight arrow*) is visible where it originates from the posterior wall of the internal carotid artery distal to the origin of the PComA (*A, curved arrow*). On the left side, the PComA and the cisternal segment of the AChA can be seen (*straight arrow, A* and *B*). The AChA is located lateral to the PComA and has a slightly smaller diameter.

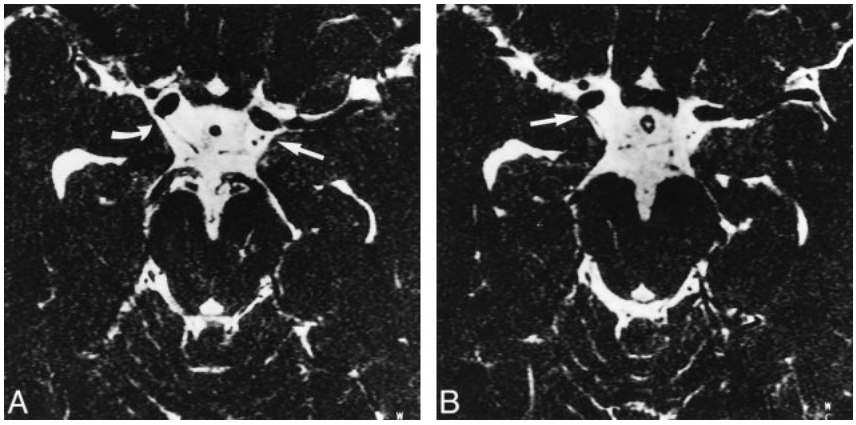

study. Additionally, three patients with AVMs had digital subtraction angiography that showed the AChA supply, which was compared with the MR findings of the AChA. Informed consent was obtained from all participants, and the study was conducted in accordance with the Declaration of Helsinki.

MR Imaging Sequences

MR studies were performed using a 1.5-T superconducting magnet with a standard circular polarized head coil. All volunteers and patients underwent MR angiography with a 3D-TOF sequence: 31/7/1 (TR/TE/excitations), slab thickness = 90 mm, number of slices = 112, effective thickness = 0.81 mm, field of view (FOV) = 200 mm, matrix = 224 × 512, flip angle = 20°. The MR angiographic source images were used for further analysis.

Ten of the 20 volunteers and one patient also underwent MR imaging with a 3D-CISS sequence: 12.3/5.9/1, slab thickness = 58 mm; number of slices = 88, effective thickness = 0.66 mm, FOV = 180 mm, matrix = 512, phase-encoding steps = 196, flip angle = 70°. The source images, which were acquired in the transverse plane, were used for further analysis.

Image Analysis

The MR studies were analyzed by two neuroradiologists. In each hemisphere, we first identified the posterior communicating artery (PComA), then the origin of the AChA, its cisternal course, and its point of entry into the temporal horn through the choroidal fissure (plexal point). We also noted whether the course of the artery could be identified in the temporal horn of the lateral ventricle. If identified, we compared the diameter of the PComA with that of the AChA.

We used an arbitrary scoring system (8) to record whether an anatomic structure was identified with certainty (score = 2), most probably identified (score = 1), or not identified (score = 0).

Results

Subjects

In the 20 healthy subjects (n = 40 hemispheres) examined with the TOF sequence, the PComA was identified with certainty (score = 2) in 87.5% (n = 35) and the AChA was identified with certainty in 92.5% (n = 37) (Fig 1). Using the 3D-CISS sequence, in the 10 subjects examined (n = 20 hemispheres) the PComA was identified with certainty in 95% (n = 19) and the AChA in 90% (n = 18) (Fig 2). The results are detailed in the Table.

In all cases in which the origin of the AChA was identified, the artery was found to originate from

MR identification of the posterior communicating artery and the anterior choroidal artery

	Score	No. of Posterior Communicating Arteries Seen	No. of Anterior Choroidal Arteries Seen	Origin	AChA		
					Cisternal Segment	Choroidal Fissure	Ventricular Segment
3D-TOF MR Angiographic Sequences (n = 40)	0	3	3	4	3	12	31
	1	2	0	7	1	3	3
	2	35	37	29	36	25	6
3D-CISS Sequences (n = 20)	0	1	1	1	2	11	19
	1	0	1	2	3	0	1
	2	19	18	17	15	9	0

Note.—The posterior communicating artery (PComA) and the anterior choroidal artery (AChA) were identified in healthy volunteers using a 3D time-of-flight MR angiographic (3D-TOF) sequence (n = 40 hemispheres studied) and a 3D Fourier transformation constructive interference in steady state (3D-CISS) sequence (n = 20 hemispheres studied). The AChA findings were further subdivided to document whether the artery was identified at its origin, in the basal cisterns, at the choroidal fissure, or in the lateral ventricles. An arbitrary scoring system was used to record whether a vessel was identified with certainty (score = 2), most probably identified (score = 1), or not identified (score = 0).

the posterior wall of the internal carotid artery distal to the PComA and proximal to the intracranial carotid bifurcation. We did not find duplications of the AChA. Neither with the TOF sequence nor the 3D-CISS sequence was it possible to depict branches originating from the artery. On average, the course of each AChA could be depicted on five to 16 (mean, 8.7) images.

In all cases in which both the PComA and the AChA were identified, the PComA had a larger diameter than the AChA. Using the 3D-TOF sequence, we found maximum diameters of 2.2 mm (PComA) and 1.25 mm (AChA) in the healthy subjects. Generally, the diameters obtained using the 3D-CISS sequence were slightly smaller, with maximum diameters of 1.9 mm (PComA) and 0.8 mm (AChA).

In general, the 3D-TOF and 3D-CISS sequences were comparable with respect to identification rates for the PComA and AChA. An exception was the region of the choroidal fissure and the temporal horn of the lateral ventricle, where the AChA was detected more often using the 3D-TOF sequence (see Table). However, the 3D-CISS sequence gave additional information in six cases: the PComA was identified with certainty (score = 2) on 3D-CISS images in three cases in which it was not identified (n = 1) or identified most probably (n = 2) on 3D-TOF images; the choroidal fissure segment of the AChA was identified with certainty (score = 2) on 3D-CISS images in two cases in which it was not identified on 3D-TOF images; and the origin of the AChA was identified with certainty (score = 2) on 3D-CISS images in one case in which it was most probably identified on 3D-TOF images.

Patients

In all three patients, the AVM supplying the AChA was enlarged and identified with certainty (score = 2) along its complete course on both the TOF (n = 3) and the 3D-CISS (n = 1) sequences (Fig 3). The AChA was identified by its origin distal to the PComA, its characteristic course along the medial surface of the temporal pole, and its entry into the choroidal fissure to reach the choroid plexus in the temporal horn. A comparison of the maximum intensity projection images with those obtained by digital subtraction angiography revealed no difference in the visualization of the anatomic course between the two methods. In contrast to the healthy volunteers, in all three patients the enlarged AChA supplying the AVM had a larger diameter than the PComA.

Discussion

To the best of our knowledge, this is the first study investigating the role of MR imaging in the identification of the AChA. Despite the small diameter of the AChA, which is usually less than 1.0 mm (0.5–2.0 mm) (9, 10), we were able to identify the artery in 37 of 40 cases by using one or both MR techniques.

Origin

The AChA regularly originates from the posterior wall of the internal carotid artery (C4) 2 to 5 mm distal to the PComA and 2 to 5 mm proximal to the carotid bifurcation (9, 11). In more recent studies, the AChA was reported to originate from the internal carotid artery in 96% to 99.5% of cases (9, 11, 12). Occasionally, the AChA has been found to arise from the intracerebral carotid bifurcation or from the PComA (1, 2, 9, 11–15). A few authors, all of whom used macroscopic rather than microscopic techniques of investigation, have reported a high percentage of cases (2.5% to 58.5%) in which the AChA originated from the middle cerebral artery (1, 15, 16). This was not confirmed in microsurgical series and may be due to differences in investigative techniques or to the confusion of the

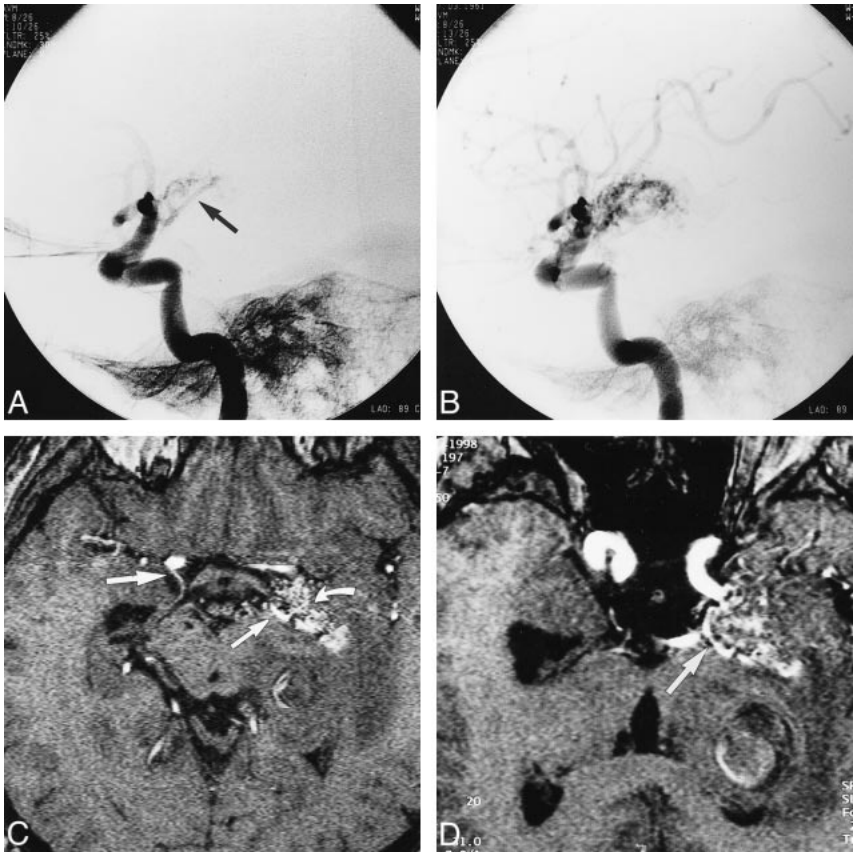

FIG 3. *A* and *B,* Lateral projections of left internal carotid artery in a 37-year-old male patient with headaches show the AVM supplied by an enlarged left AChA (*arrow, A*).

C, Axial MR angiographic source image obtained using a 3D-TOF sequence (31/7/1) shows areas of the AVM with high blood flow (*curved arrow*), the origin of the patient's right AChA (*large straight arrow*), and enlargement of the left AChA (*small straight arrow*) that supplies the AVM.

D, Reconstructed MR angiographic image oriented along the axis of the cisternal course of the left AChA shows the entire cisternal course of the left AChA (*arrow*).

AChA with the uncal artery, which may arise from the proximal segment of the middle cerebral artery (9, 12). In all cases in which we were able to identify the origin of the AChA, it arose from the posterior wall of the internal carotid artery distal to the PComA and proximal to the intracranial carotid bifurcation. In three of 40 hemispheres (7.5%), we could not identify the artery. Since absence of the artery is considered to be exceedingly rare (11), it is possible that in these cases the diameter of the vessel was too small to be detected by MR imaging.

The prevalence of duplication of the AChA remains controversial. Saeki and Rhoton (2) found a duplication in 4% of cases. Yasargil (9) reported that in 30% of cases the AChA arose as two to four independent vessels; in the remaining 70% of cases, the AChA originated as a single trunk that usually then divided either immediately or within 2 to 5 mm into two trunks. On the other hand, Morandi et al (12) and Lasjaunias and Berenstein (17) considered this merely a pseudoduplication with separation of the origin of the uncal artery. They considered true duplication of the AChA to be a rarity. We did not find any duplications of the AChA, although we may have missed possible additional trunks if they had very small diameters.

Course

The course of the AChA can be divided into two segments, the cisternal and the intraventricular. The length of the cisternal segment ranges from 15 to 35 mm (mean, 26 mm) (18). In this segment, the AChA has a complex relationship to the optic tract, which changes along its course. At its origin, the AChA is located lateral to the optic tract, then it curves medially to the inferomedial surface, to curve again laterally running along the lateral aspect of the optic tract to reach the lateral geniculate body. The AchA then passes through the choroidal fissure to reach the choroid plexus of the temporal horn. The terms plexal point or ventral choroidal point have been proposed to describe the point of entry of the AChA into the lateral ventricle at the choroidal fissure (12). The artery passes over the medial surface of the temporal horn, curving around the atrium to the floor of the body of the lateral ventricle. Within the collateral trigone the AChA anastomoses with the posterior choroid artery.

In our study, we were able to follow the course of the AChA through the basal cisterns (carotid, crural, ambient cistern) to the choroidal fissure in most cases (see Table). Using the 3D-TOF MR angiographic sequence, we could even identify the artery in the lateral ventricle in a few cases (n = 6). Obviously, the diameters of the branches of the AChA are too small to be detected by MR imaging.

Angiographic Findings

The AChA is not always visible on conventional angiograms, either because of its small diameter or

because it is obscured by branches of the middle cerebral artery. In the literature, the frequency of angiographic visualization of this artery has been reported to be between 71% and 98% (18).

Some of the branches of the AChA can be identified on lateral angiograms. In the proximal half of the cisternal segment, ascending branches that course into the region of the globus pallidus and internal capsule are seen frequently. More posteriorly, small descending branches to the uncus may be noted. In the terminal portion of the cisternal segment, additional ascending branches that supply the region of the lateral geniculate body, posterior limb of the internal capsule, and retrolenticular area may be identified (10). Angiographic identification of the uncal artery and of perforating branches has been reported in 36% and 47% of cases, respectively (19).

On lateral angiograms, the plexal point, where the artery enters the choroid plexus, is at a distance of 18 to 26 mm from the origin of the AChA. This important angiographic landmark is usually characterized by a steep downward course of a few millimeters, followed by a sharp posterior turn, marking the point of entry.

MR Imaging of the AChA

In the data presented in our report, MR imaging using a 3D-TOF MR angiographic sequence allowed identification of the AChA with certainty in 95% of cases. This compares well with the rates of identification reported in studies using conventional angiography (18). In our opinion, MR angiography thus represents a useful, noninvasive alternative for screening the AChA. Visualization of the AChA may be clinically important if an involvement of the artery is suspected in cases of infarctions, intracranial aneurysms, AVMs, or intracranial tumors. The anatomic features that help to identify the artery on the MR angiographic source images are 1) its typical point of origin from the posterior wall of the internal carotid distal to the PComA and proximal to the intracerebral carotid bifurcation, and 2) its characteristic posterior course, especially when it runs along the medial aspect of the uncus to curve laterally along the medial aspect of the temporal lobe (ambient gyrus) through the ambient cistern to the choroidal fissure (Fig 4).

In general, we found that identification of the AChA was easier using the 3D-TOF than the 3D-CISS sequence, most probably because of the high signal of the arteries in the former as compared with the latter sequence. However, in selected cases, the 3D-CISS sequence may give additional information, especially if combined with MR angiography. The 3D-CISS sequence is helpful in visualizing fine structures located in the cisterns (7, 20) and will probably give a more realistic measure of the diameter of the AChA than the 3D-TOF sequence. But the 3D-CISS sequence is only helpful when the structures to be identified are surrounded by CSF (7). As soon as the CSF layer disappears, as happens when the artery is adjacent to the brain surface, identification of the artery becomes quite difficult. Furthermore, since all cisternal structures, such as arteries, veins, and nerves, have the same signal intensity on 3D-CISS images, these structures can only be differentiated by following their course anatomically from the origin to the end (7). In contrast, arteries are easily identified by their bright signal when using the 3D-TOF sequence.

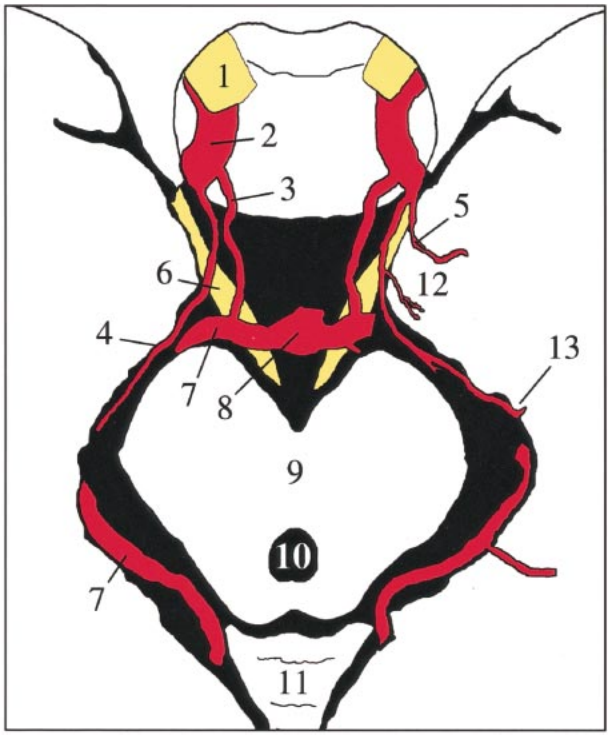

FIG 4. Schematic drawing of an axial cut through the midbrain. The AChA (*4*) originates from the internal carotid artery (*2*), runs toward the medial aspect of the uncus (*12*), and then curves laterally along the medial aspect of the temporal lobe through the ambient cistern to the choroidal fissure (*13*). The uncal artery on the left has a common origin with the AChA. *1,* optic nerve; *2,* internal carotid artery; *3,* PComA; *4,* AChA; *5,* uncal artery; *6,* oculomotor nerve; *7,* posterior cerebral artery; *8,* tip of the basilar artery; *9,* mesencephalon; *10,* aqueduct of Sylvius; *11,* cerebellum; *12,* uncus of the temporal lobe; *13,* choroidal fissure.

While the 3D-CISS sequence depicts the external contour of the AChA, the 3D-TOF sequence shows flow within the vessel. Thus, using both sequences, it may be possible to discriminate hypoplasia of the vessel from occlusion in suspected cases of infarction or vasculitis. In our study, certain segments of the AChA were not identified on the 3D-TOF images but were definitely identified on the 3D-CISS images in three arteries. As other segments of the AChA were well visualized on the 3D-TOF images, we assume that the artery was not occluded, but rather that the flow within the artery was below the level of detection by the 3D-TOF sequence we used. Absence of flow signal is therefore only one aspect that has to be taken into consideration when examining patients with arterial diseases.

In contrast to the volunteers we studied, the AChA supplying an AVM was larger than the PcomA in all three patients with an AVM. However, this may not necessarily be the situation in many cases of the AChA supply an AVM, particularly when there is a dominant PComA because of congenital hypoplasia of the P1 segment on that side.

In our study, MR angiography was not able to depict branches of the AChA, presumably because of their small diameter. However, when the AChA supplies tumors or AVMs, it usually enlarges. In these cases, identification of the artery by MR imaging is easier, as demonstrated in the three patients in whom the AChA was clearly identified. In these cases, MR imaging may thus be a useful method for follow-up examinations, such as after gamma-knife treatment of an AVM.

Conclusion

The AChA can be reliably identified using both a 3D-CISS sequence as well as source images of a 3D-TOF sequence. Anatomic features that help to identify the artery on MR angiographic source images are its typical point of origin from the posterior wall of the internal carotid distal to the PComA and proximal to the intracerebral carotid bifurcation, and its characteristic posterior course, especially when it runs along the medial aspect of the uncus to curve laterally along the medial aspect of the temporal lobe through the ambient cistern to the choroidal fissure. Identification of the AChA was easier using the 3D-TOF than the 3D-CISS sequence. In selected cases, however, the 3D-CISS sequence may give additional information and may be combined with MR angiography. MR imaging is a useful noninvasive alternative for screening the AChA and can be used to assess and follow up AChA-related disorders, especially AVMs.

Acknowledgment

The advice of U. D. Schmid is gratefully acknowledged.

References

1. Carpenter MR, Noback CR, Moss ML. **The anterior choroidal artery: its origin, course distribution and variations.** *Arch Neurol Psychiatry* 1954;71:714–722
2. Saeki N, Rhoton AL. **Microsurgical anatomy of the upper basilar artery and the posterior circle of Willis.** *Neurosurgery* 1977;46:563–578
3. Helgason CM. **A new view of anterior choroidal artery territory infarction.** *J Neurol* 1988;235:387–391
4. Pullicino PM. **The course and territories of cerebral small arteries.** *Adv Neurol* 1993;62:11–39
5. Foix C, Chavany JA, Hillemand P, Schiff-Wertheimer S. **Oblitération de l'artère choroidienne antérieure: ramollissement de son territoire cérébral: hémiplégie, hémianesthésie, hémianopsie.** *Bull Soc Ophtalmol Paris* 1925;37:221–223
6. Leys D, Mounier-Vehier F, Lavenu I, Rondepierre P, Pruvo JP. **Anterior choroidal artery territory infarcts: study of presumed mechanisms.** *Stroke* 1994;25:837–842
7. Yousry I, Camelio S, Wiesmann M, et al. **Detailed magnetic resonance imaging anatomy of the cisternal segment of the abducens nerve: Dorello's canal and neurovascular relationships and landmarks.** *J Neurosurg* 1999;91:276–283
8. Yousry TA, Schmid UD, Alkadhi H, et al. **Localization of the motor hand area to a knob on the precentral gyrus: a new landmark.** *Brain* 1997;120:141–157
9. Yasargil MG. ***Microneurosurgery.*** Stuttgart: Thieme;1984:66–70
10. Goldberg HI. **The anterior choroidal artery.** In: Newton TH, Potts DC, eds. *Radiology of the Skull and Brain: Angiography*. St Louis: Mosby;1974:1628–1658
11. Otomo E. **The anterior choroidal artery.** *Arch Neurol* 1965;13:656–658
12. Morandi X, Brassier G, Darnault P, Mercier P, Scarabin JM, Duval JM. **Microsurgical anatomy of the anterior choroidal artery.** *Surg Radiol Anat* 1996;18:275–280
13. Herman LH, Fernando OV, Gurdjian ES. **The anterior choroidal artery: an anatomical study of its area of distribution.** *Anat Rec* 1966;154:95–102
14. Hussein S, Renella RR, Dietz H. **Microsurgical anatomy of the anterior choroidal artery.** *Acta Neurochir (Wien)* 1988;92:19–28
15. Mitterwallner F. **Variationsstatistische Untersuchungen an den basalen Hirngefässen.** *Acta Anat (Basel)* 1955;24:51–88
16. Cavatorti P. ***Das Arteriensystem der Japaner.*** Kyoto: Marysen;1928:112–113
17. Lasjaunias P, Berenstein A. ***Surgical Neuroangiography, 3: Functional Anatomy of Brain Spinal Cord and Spine.*** Berlin: Springer;1990:160
18. Huber P. ***Cerebral Angiography.*** Stuttgart: Thieme;1982:75–79
19. Takahashi S, Suga T, Kawata Y, Sakamoto K. **Anterior choroidal artery: angiographic analysis of variations and anomalies.** *AJNR Am J Neuroradiol* 1990;11:719–724
20. Yousry I, Camelio S, Schmid UD, Horsfield MA, Wiesmann M, Brückmann H, Yousry TA. **Visualization of cranial nerves I–XII: value of 3D CISS and T2-weighted sequences.** *Eur Radiol* 2000;10:1061–1067